Simultaneous Measurement of Protein Oxidation and *S*-Nitrosylation During Preconditioning and Ischemia/Reperfusion Injury With Resin-Assisted Capture

Mark J. Kohr, Junhui Sun, Angel Aponte, Guanghui Wang, Marjan Gucek, Elizabeth Murphy, Charles Steenbergen

Rationale: **Redox modifications play an important role in many cellular processes, including cell death. Ischemic preconditioning (IPC) has been shown to involve redox signaling. Protein *S*-nitrosylation (SNO) is increased following myocardial IPC, and SNO is thought to provide cardioprotection, in part, by reducing cysteine oxidation during ischemia/reperfusion (IR) injury.**

Objective: **To test the hypothesis that SNO provides cardioprotection, in part, by shielding against cysteine oxidation following IR injury.**

Methods and Results: **We developed a new method to measure protein oxidation using resin-assisted capture (Ox-RAC), which is similar to the SNO-RAC method used in the quantification of SNO. Langendorff-perfused hearts were subjected to various perfusion protocols (control, IPC, IR, IPC-IR, IPC/reperfusion) and homogenized. Each sample was divided into 2 equal aliquots, and the SNO-RAC/Ox-RAC procedure was performed to simultaneously analyze SNO and oxidation. We identified 31 different SNO proteins with IPC, 27 of which showed increased SNO compared to baseline. Of the proteins that showed significantly increased SNO with IPC, 76% showed decreased oxidation or no oxidation following ischemia and early reperfusion (IPC-IR) at the same site when compared to IR alone; for non-SNO proteins, oxidation was reduced by only 50%. We further demonstrated that IPC-induced protein SNO is quickly reversible.**

Conclusions: **These results support the hypothesis that IPC-induced protein SNO provides cardioprotection by shielding cysteine residues from reactive oxygen species–induced oxidation during IR injury. Therefore, the level of protein SNO plays a critical role in IR injury, where ROS production is increased. (*Circ Res*. 2011;108:00-00.)**

Key Words: ischemic preconditioning ■ *S*-nitrosothiol ■ reactive oxygen species

The interplay between reactive oxygen species (ROS) and nitric oxide (NO), referred to as the nitroso-redox balance, is critical in the regulation of myocardial function. Redox modified protein thiols are known to alter the function of key proteins in the myocardium, including the L-type Ca^{2+} channel,[1] the sarcoplasmic reticulum Ca^{2+}-ATPase,[2,3] and the sarcoplasmic reticulum Ca^{2+} release channel (RyR2).[4,5] RyR2 appears to be particularly sensitive to redox modification, such that the interplay between protein *S*-nitrosylation and oxidation appears to be crucial in regulating channel activity. The nitroso-redox balance is also critically important during the setting of ischemia/reperfusion (IR) injury, which results in widespread thiol oxidation as a consequence of the burst of ROS that occurs in the first few minutes of reperfusion following ischemia. The end result of this widespread oxidation is a nitroso-redox imbalance. Ischemic preconditioning (IPC), which develops from transient episodes of IR and renders the heart resistant to damage resulting from subsequent sustained periods of ischemia, has been shown to involve redox signaling.[6] Furthermore, IPC has been shown to reduce the initial burst of ROS, and oxidative stress is thought to be important in cell death.[7]

NO has been shown to play a key role in cardioprotection.[8] The cGMP-dependent effects of NO in IPC are well documented and occur via activation of the mitochondrial K_{ATP} channel.[9] cGMP-independent effects of NO also play a significant role in cardioprotection.[2,10,11] Treatment with the *S*-nitrosylating agent *S*-nitrosoglutathione increases protein *S*-nitrosylation and induces cardioprotection.[2] *S*-Nitrosylation is a reversible, redox-dependent protein modification in which an NO moiety is covalently attached to the free thiol of a cysteine residue.[12–14] This modification has been demon-

Original received September 10, 2010; revision received December 21, 2010; accepted December 21, 2010. In November 2010, the average time from submission to first decision for all original research papers submitted to *Circulation Research* was 13.2 days.

From the Department of Pathology (M.J.K., C.S.), Johns Hopkins Medical Institutions, Baltimore; and Systems Biology Center (M.J.K., J.S., E.M.) and Proteomics Core Facility (A.A., G.W., M.G.), National Heart, Lung, and Blood Institute, NIH, Bethesda, MD.

Correspondence to Charles Steenbergen, Department of Pathology, Johns Hopkins Medical Institutions, 632 N Ross Research Building, 720 Rutland Ave, Baltimore, MD 21257. E-mail csteenb1@jhmi.edu

Circulation Research **is available at http://circres.ahajournals.org** **DOI: 10.1161/CIRCRESAHA.110.232173**

Non-standard Abbreviations and Acronyms

DEPC	diethyl pyrocarbonate
DIGE	difference gel electrophoresis
DTT	dithiothreitol
IPC	ischemic preconditioning
IPC-IR	ischemic preconditioning–ischemia/reperfusion
IPC-R	ischemic preconditioning/reperfusion
IR	ischemia/reperfusion
LC-MS/MS	liquid chromatography–tandem mass spectrometry
MMTS	methyl methanethiosulfonate
MS	mass spectrometry
NEM	*N*-ethylmaleimide
Ox	oxidation
RAC	resin-assisted capture
ROS	reactive oxygen species
RYR2	sarcoplasmic reticulum Ca^{2+} release channel
SNO	*S*-nitrosylation

strated to modify the activity of target proteins.[1,2,15] Protein targets which have been shown to be *S*-nitrosylated include aconitate hydratase, aldehyde dehydrogenase, α-ketoglutarate dehydrogenase, mitochondrial complex I, creatine kinase, F_1F_0-ATPase, malate dehydrogenase, sarcoplasmic reticulum Ca^{2+}-ATPase, and thioredoxin.[2,11,16,17]

S-Nitrosylation is also proposed to protect cysteine residues against potential oxidative damage from ROS.[18–20] Many ROS-induced protein modifications are irreversible, and if they alter protein function and/or denature proteins, this will lead to a period of sustained myocardial dysfunction following IR injury. Because *S*-nitrosylation is a transient modification, *S*-nitrosylation of proteins during IPC could shield cysteine residues from irreversible oxidation during the first few minutes of reperfusion, after which time, the *S*-nitrosylation is removed and normal protein function can resume. At this point, the initial burst of ROS is complete and the protein is protected from oxidative damage. Thus, the level of *S*-nitrosylation could play a critical role in IR injury, when ROS production is increased.[21]

Therefore, it is of interest to determine whether *S*-nitrosylation can exert cardioprotective effects by reducing cysteine oxidation (Figure 1A). To test this hypothesis, the simultaneous measurement and site identification of both *S*-nitrosylation and oxidation is required. Forrester et al recently published a technique for measuring and identifying the sites of protein *S*-nitrosylation (SNO-RAC).[22] Herein, we describe a new protocol based on the SNO-RAC method, for the measurement and site determination of protein cysteine oxidation (Ox-RAC). This newly developed protocol, when performed in tandem with the SNO-RAC technique, provides the methods necessary to address the important question of whether IPC-induced protein *S*-nitrosylation shields critical cysteine residues against oxidation.

Methods

An expanded Methods section is available in the Online Data Supplement at http://circres.ahajournals.org.

Animals

Male C57BL/6 mice (12 to 15 weeks) were obtained from The Jackson Laboratory (Bar Harbor, ME). This investigation conforms to the *Guide for the Care and Use of Laboratory Animals* (NIH publication no. 85-23, revised 1996) and was approved by the Institutional Laboratory Animal Care and Use Committee.

Perfusion Protocols, Whole-Heart Homogenate Preparation, and Enzyme Assays

Hearts were Langendorff-perfused as described previously[2,23] and snap-frozen in liquid nitrogen immediately following the treatment protocol; treatment protocols are shown in Figure 1B. Whole-heart homogenate preparations[2,23] and GAPDH activity measurements[24] were performed as described previously.

Oxidation Site Identification With Resin-Assisted Capture

For oxidation site identification (Ox-RAC; Figure 1C), samples (1 mg) were diluted in HEN buffer containing (in mmol/L): HEPES-NaOH 7.7 (250), EDTA (1), and neocuproine (0.1) with 2.5% SDS and an EDTA-free protease inhibitor tablet (Roche Diagnostics Corp, Indianapolis, IN). All buffers were degassed before use to

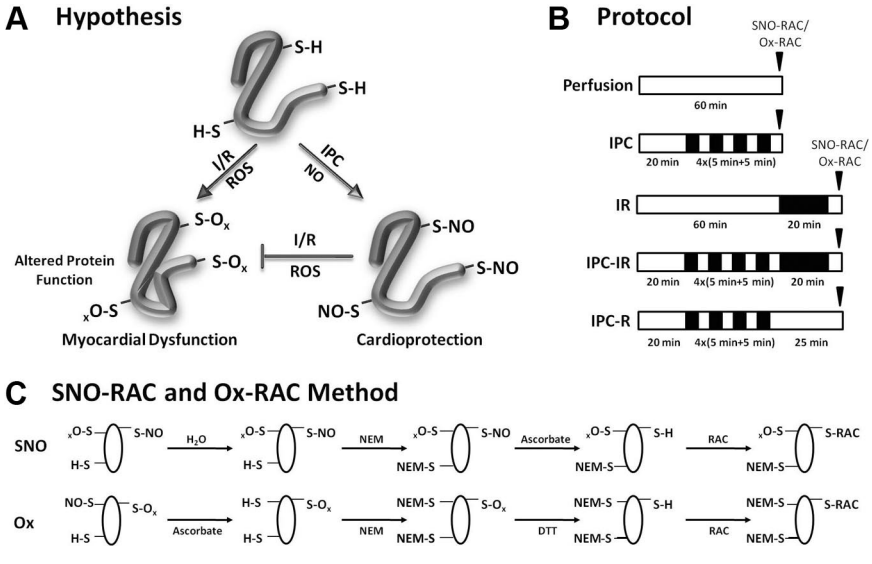

Figure 1. Hypothesis, treatment protocols, and methodology. A, ROS production increases during IR injury, leading to irreversible cysteine oxidation (O_x) and myocardial dysfunction **(left)**. Conversely, SNO increases during IPC, leading to cardioprotection via direct block against cysteine oxidation **(right)**. **B,** Hearts were randomly subjected to 1 of 5 perfusion protocols. Periods of perfusion and ischemia are indicated by **white and black boxes**, respectively. **C,** A modified version of the biotin switch protocol was used to identify *S*-nitrosylated (SNO) and oxidized (Ox) proteins with RAC.

prevent oxidation of the resin. Homogenates were then incubated with 20 mmol/L ascorbate (Sigma, St Louis, MO) for 45 minutes at room temperature to remove SNO. The inclusion of this step serves to distinguish SNO from other oxidative modifications; this step can be eliminated for the combined examination of SNO and other oxidative modifications. Samples were then incubated with 50 mmol/L *N*-ethylmaleimide (NEM) (Sigma) for 20 minutes at 50°C to block unmodified (ie, free) and ascorbate-reduced thiol groups from modification; ascorbate and NEM were removed via acetone precipitation. Samples were then resuspended in HEN with 1% SDS (HENS) and oxidized thiols were reduced with 10 mmol/L dithiothreitol (DTT) (Pierce, Rockford, IL) for 10 minutes at room temperature; DTT was removed via acetone precipitation. Samples were then resuspended in HENS. Thiopropyl sepharose (GE Healthcare, Piscataway, NJ) was rehydrated for 25 minutes in diethyl pyrocarbonate (DEPC) H_2O. Following rehydration, 25 μL of the resin slurry was added to a Handee Mini Spin Column (Pierce) and washed with 5×0.5 mL of DEPC H_2O, followed by 10×0.5 mL of HEN buffer. Blocked samples were then added to the thiopropyl sepharose-containing spin column and rotated for 4 hours in the dark at room temperature. Proteins bind to the resin by forming disulfide linkages between reduced thiol groups of the protein and the thiol groups of the resin. Resin-bound proteins were then washed with 8×0.5 mL of HENS buffer, followed by 4×0.5 mL of HENS buffer diluted 1:10. Samples were then subjected to trypsin digestion (sequencing grade modified; Promega, Madison, WI) overnight at 37°C with rotation in buffer containing (in mmol/L): NH_4HCO_3 (50) and EDTA (1). Resin-bound peptides were then washed with 5×0.5 mL of HENS buffer diluted 1:10, 5×0.5 mL of 2 mol/L NaCl, 5×0.5 mL of 80% acetonitrile/0.1% trifluoroacetic acid, and 5×0.5 mL of HEN buffer diluted 1:10. Peptides were eluted for 30 minutes at room temperature in elution buffer containing (in mmol/L): DTT (20), NH_4CO_3 (10), and 50% methanol. The resin was then washed with an additional volume of elution buffer, followed by 2 volumes of DEPC water. All fractions were combined and concentrated via SpeedVac. Samples were then resuspended in 0.1% formic acid and cleaned with a C_{18} column (ZipTip; Millipore, Billerica, MA). Liquid chromatography–tandem mass spectrometry (LC-MS/MS) was then performed using an LTQ Orbitrap XL mass spectrometer (Thermo Fisher Scientific, San Jose, CA). The MASCOT database search engine was used for protein identification. Relative quantification of SNO and oxidation was performed using an in-house software program designed as a label-free approach to peptide quantification by LC-MS/MS.[25]

S-Nitrosylation Site Identification With Resin-Assisted Capture

A modified version of the SNO-RAC protocol was used to examine protein SNO (Figure 1C).[22] Briefly, samples (1 mg) were diluted in HEN buffer with 2.5% SDS and an EDTA-free protease inhibitor tablet (Roche Diagnostics Corporation). All buffers were degassed before use to prevent oxidation of the resin. Homogenates were then incubated with 50 mmol/L NEM for 20 minutes at 50°C to block unmodified (ie, free) thiol groups from modification; NEM was removed via acetone precipitation. Samples were then resuspended in HENS and subjected to the same procedure as described above for the Ox-RAC protocol, with the exception that samples were not reduced with DTT and were coincubated with thiopropyl sepharose and 20 mmol/L ascorbate to reduce SNO.

Statistics

Statistical significance ($P<0.05$) was determined between groups using ANOVA for multiple groups or Student *t* test for 2 groups.

Results

To test whether *S*-nitrosylation (SNO) provides transient protection of cysteine residues against oxidation, we developed the oxidation resin-assisted capture (Ox-RAC) protocol for the measurement and site identification of protein oxidation, and used this in tandem with the SNO-RAC method (see Figure 1C).[22] The Ox-RAC protocol uses a combination of procedures adapted from the SNO-RAC method and redox difference electrophoresis (redox DIGE).[26] We made several modifications to the original SNO-RAC method so that it would be better suited for use in combination with the Ox-RAC protocol. These changes included the use of *N*-ethylmaleimide (NEM) rather than methyl methanethiosulfonate (MMTS) as a blocking agent. This substitution was made because MMTS is susceptible to DTT reduction during the step in which peptides are eluted from the resin. Conversely, NEM is not affected by DTT. This is particularly important with peptides that contain multiple cysteine residues; unmodified cysteine residues (ie, not SNO or oxidized) will remain blocked with NEM and will be detected as such by mass spectrometry, thus allowing us to distinguish unmodified cysteine residues from SNO or oxidized cysteine residues (which will not be labeled with NEM) in the case of peptides that have multiple cysteines. The MMTS would be removed by DTT during the elution step and unmodified cysteine residues would not be distinguishable from SNO or oxidized cysteine residues in peptides with multiple cysteines.

As a negative control for the Ox-RAC protocol, whole-heart homogenates were pretreated with ascorbate and blocked with NEM. Non-DTT-reduced samples were then incubated with the resin, subjected to trypsin digestion, and analyzed via LC-MS/MS. Only 1 cysteine-containing peptide was detected by LC-MS/MS, indicating that ascorbate pretreatment is effective at reducing *S*-nitrosylation, and that NEM is effective at blocking both unmodified and ascorbate-reduced thiol groups. These data also demonstrate that DTT-dependent false-positive signals with the Ox-RAC protocol are extremely low. Furthermore, the use of a higher concentration of ascorbate (50 mmol/L) yielded similar results to that observed with 20 mmol/L ascorbate. Identifications from nonspecifically bound peptides (ie, non–cysteine-containing peptides) accounted for ≈6% of all peptide identifications; non–cysteine-containing peptides were filtered from the data set. These data demonstrate that the SNO-RAC and Ox-RAC techniques are very specific for the identification of SNO and oxidized cysteine residues, respectively.

IPC Transiently Increases Protein *S*-Nitrosylation

Using the modified SNO-RAC protocol, we identified a total of 33 unique SNO proteins (47 sites corresponding to 39 peptides; note some proteins have multiple peptides and/or multiple cysteines on the same peptide) among the 4 perfusion protocols (see Table 1 and Figure 2A). We identified 11 proteins at baseline, an additional 20 SNO proteins with IPC, and 2 additional SNO proteins with IPC-IR. All 11 of the SNO proteins observed at baseline were also found with IPC, along with 20 additional proteins for a combination of 31 SNO proteins (45 sites corresponding to 37 peptides). Label-free peptide analysis was performed for the 11 common proteins comparing baseline and IPC, and we determined that seven of eleven proteins showed a significant increase in SNO with IPC compared to baseline. Note that this includes isocitrate dehydrogenase [NADP], which had one peptide detected at baseline that did not show a significant increase

Table 1. Peptides Showing Cysteine *S*-Nitrosylation As Identified via SNO-RAC Proteomic Analysis

				Perfusion		IPC		IR		IPC-IR	
Protein Name	Protein ID	Peptide Sequence	SNO Cys	Ratio	Ion Score	Ratio	Ion Score	Ratio	Ion Score	Ratio	Ion Score
Citrate synthase (M)	Q9CZU6	GYSIPECQK	101	1	37	3.29	30	0.43*	30		
Cytochrome *b*–*c*1 complex subunit 1 (M)	Q9CZ13	VYEEDAVPGLTPCR	268				79				
		LCTSATESEVTR	380	1	81	7.31*	77			3.30*	92
Fructose-bisphosphate aldolase A	P05064	ALANSLACQGK	339	1	83	9.90*	90	1.70*†	80	10.00*‡	81
Glyceraldehyde-3-phosphate dehydrogenase	P16858	IVSNASCTTNCLAPLAK	150, 154	1	124	2.97*	122	0.07*†	126	1.34†‡	129
		VPTPNVSVVDLTCR	245	1	105	2.10*	98			0.90†	101
Isocitrate dehydrogenase [NADP] (M)	P54071	SSGGFVWACK	308				62				
		VCVQTVESGAMTK	402	1	116	1.91	112			1.01†	109
L-lactate dehydrogenase A chain	P06151	IVSSKDYCVTANSK	84				51				
		VIGSGCNLDSAR	163	1	96	3.81*	86				
Malate dehydrogenase	P14152	VIVVGNPANTNCLTASK	137	1	113	0.61*	126			0.70	115
Malate dehydrogenase (M)	P08249	EGVVECSFVQSK	275	1	60	1.16	76			1.22	67
Protein NipSnap homolog 2	O55126	ICQEVLPK	89	1	55	22.40*	53	0.30*†	54	9.91*†‡	58
Succinyl-CoA ligase α (M)	Q9WUM5	IICQGFTGK	60	1	40	0.71	48	0.23*†	43	0.63	45
Triosephosphate isomerase	P17751	IAVAAQNCYK	67	1	59	3.40*	62	0.44*†	53	1.42*‡	43
		IIYGGSVTGATCK	218				103				107
Aconitate hydratase (M)	Q99KI0	VGLIGSCTNSSYEDMGR	385				124				102
Aspartate aminotransferase	P05201	INMCGLTTK	391				57				
Aspartate aminotransferase (M)	P05202	VGAFTVVCK	295				44				48
β-enolase	P21550	VNQIGSVTESIQACK	357				101				
Cysteine and glycine-rich protein 3	P50462	TVYHAEEIQCNGR	25				73				41
Cysteine-rich protein 2	Q9DCT8	ASSVTTFTGEPNMCPR	126				76				
Cytochrome c oxidase subunit 5b (M)	P19536	cPNCGTHYK	115				30				
Electron transfer flavoprotein subunit α (M)	Q99LC5	TIYAGNALCTVK	155				80				
Electron transfer flavoprotein subunit β (M)	Q9DCW4	EIIAVSCGPSQCQETIR	66, 71				103				
Enoyl-CoA hydratase (M)	Q8BH95	LVEEAIQCAEK	225				80				
Isocitrate dehydrogenase [NAD] subunit α (M)	Q9D6R2	IEAACFATIK	331				30				
Long-chain-fatty-acid-CoA ligase 1	P41216	GIQVSNNGPCLGSR	109				72				
Metallothionein-1	P02802	SCCSCCPVGCSK	33, 34, 36, 37, 41				45				
		GAADKCTCCA	57, 59, 60				49				
NADH dehydrogenase [ubiquinone] 1 α subcomplex subunit 10 (M)	Q99LC3	VITVDGNICSGK	67				69				
Peroxiredoxin-6	O08709	DFTPVCTTELGR	47				44				
Propionyl-CoA carboxylase α chain	Q91ZA3	MADEAVCVGPAPTSK	107				95				
Succinate dehydrogenase [ubiquinone] flavoprotein (M)	Q8K2B3	VGSVLQEGCEK	536				51				

(Continued)

Table 1. Continued

Protein Name	Protein ID	Peptide Sequence	SNO Cys	Perfusion Ratio	Perfusion Ion Score	IPC Ratio	IPC Ion Score	IR Ratio	IR Ion Score	IPC-IR Ratio	IPC-IR Ion Score
Succinyl-CoA ligase subunit β (M)	Q9Z2I9	ILAC̲DDLDEAAK	430				68				
Sarcoplasmic/endoplasmic reticulum calcium ATPase 2	O55143	SMSVYC̲TPNKPSR	498								44
Tubulin β-4 chain	P04350	NMMAAC̲DPR	303				48				49
Very-long-chain specific acyl-CoA dehydrogenase (M)	P50544	SSAIPSPC̲GK	238								35
Voltage-dependent anion channel protein 2 (M)	Q60930	SC̲SGVEFSTSGSSNTDTGK	48				83				86

Each protein/peptide was identified from at least 3 of 5 SNO-RAC/LC-MS/MS proteomic analyses (peptides were filtered at a false discovery rate of 5%; peptides with ion scores <30 were not accepted). M indicates mitochondrial isoform; C̲, SNO cysteine residue; c, NEM-blocked cysteine residue. Peptides not detected under the specified condition contain a blank space in the ion score column. *P<0.05 vs perfusion; †P<0.05 vs IPC; ‡P<0.05 vs IR.

and a new peptide with IPC that was significant. These SNO proteins included glyceraldehyde-3-phosphate dehydrogenase (GAPDH), lactate dehydrogenase, and triosephosphate isomerase. The remaining 4 common proteins did not show an increase in SNO with IPC compared to baseline. After 20 minutes of ischemia and 5 minutes of reperfusion, the total number of SNO proteins identified in IPC-IR samples decreased by ≈50% (16 proteins) compared to IPC alone, indicating that IPC-induced SNO formation is quickly reversible. Two of the SNO proteins (2 sites corresponding to 2 peptides) consistently observed with IPC-IR were not observed with IPC alone. Following 20 minutes of ischemia and 5 minutes of reperfusion in the absence of IPC, the total number of SNO proteins identified via SNO-RAC fell to 6 proteins and of these six proteins, 5 showed a significant decrease in SNO compared to baseline.

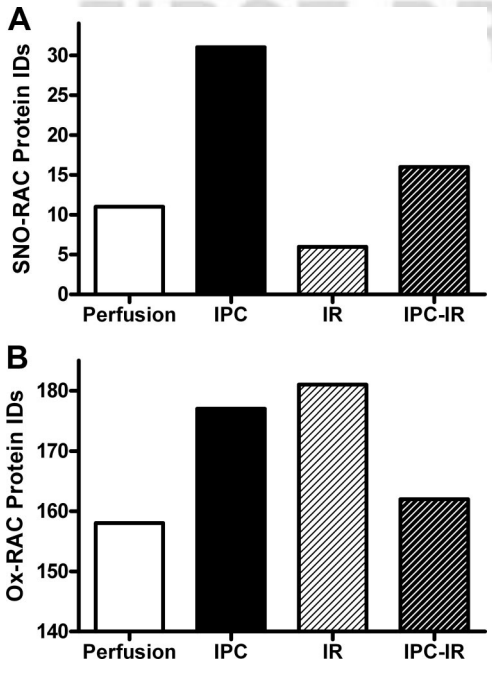

Figure 2. SNO-RAC and Ox-RAC protein identifications. Total number of proteins from SNO-RAC **(A)** and Ox-RAC **(B)**, as identified via LC-MS/MS for each treatment protocol at a false discovery rate of 5% (n=5 hearts/group).

To determine whether the reduction in protein SNO observed with IPC-IR occurred as a result of IR or was a time-dependent process, we conducted an additional set of SNO-RAC experiments. Hearts (n=5) were subjected to a perfusion protocol identical to that used for IPC-IR, with the exception that hearts were not exposed to an ischemic period (IPC-R). Instead, hearts were subjected to a post-IPC reperfusion period equal to that of the combined duration of the ischemic and reperfusion periods of the IPC-IR protocol (Figure 1B). Following 4 cycles of IPC and a 25 minute reperfusion period, the number of SNO proteins detected in IPC-R samples was similar to that observed with IPC-IR (12 proteins versus 16 proteins). This result indicates that IPC-induced protein SNO is transient and decays with time.

IPC Reduces Protein Oxidation

Using the newly developed Ox-RAC protocol, we identified a large set of oxidized proteins for each of the 4 perfusion protocols (Figure 2B). A subset of these oxidized proteins can be found in Online Table I, which shows oxidation site identifications for the same proteins identified in Table 1. As shown in Online Table II, we identified 158 proteins that showed constitutive oxidative modification at baseline. Although there are a large number of proteins with some degree of oxidation at baseline, this number includes proteins with disulfide bonds and iron-sulfur groups. There were a total of 127 proteins that showed oxidation with all 4 perfusion protocols. Following IR injury, we found 181 oxidized proteins (Online Table III); more than 35% of the common proteins between perfusion and IR showed a significant increase in protein oxidation. Interestingly, 17 unique proteins were oxidized with IR alone and were not detected in the other perfusion protocols. These 17 unique proteins may include those responsible for the detrimental effects of IR-induced oxidation. With IPC, we detected 177 oxidized proteins (Online Table IV), including 13 unique proteins that were not detected in the other perfusion protocols. A closer examination of the proteins oxidized with IPC compared to those oxidized with IR revealed that the 2 populations of

oxidized proteins were very different and, excluding proteins common among all 4 perfusion protocols (127 proteins), only 18 proteins were shared (≈35% similarity). Following IPC-IR, 162 oxidized proteins were identified (Online Table V). The drop in oxidized proteins with IPC-IR compared to IPC alone may result, in part, from the IPC-induced activation of oxidant repair mechanisms. Additionally, 138 common proteins were identified between IR and IPC-IR, and 55% of these common proteins showed a significant reduction in cysteine oxidation with IPC-IR compared to IR alone. Note that Online Tables II through V provide all protein/peptide identifications, including those detected in fewer than 3 of 5 samples.

IPC-Induced Protein *S*-Nitrosylation Provides a Direct Protective Effect Against Cysteine Oxidation Following IR Injury

Consistent with the hypothesis that SNO can provide direct protection against cysteine oxidation, we examined the oxidation state of the 27 proteins that showed a significant increase in SNO with IPC (42 sites corresponding to 34 peptides). Of these proteins, six did not show any oxidation at the sites of SNO in either IR or IPC-IR and were excluded from comparison. Of the remaining 21 SNO proteins, 76% (16 of 21 proteins) showed a significant reduction in oxidation or no oxidation at all following IPC-IR at the same site when compared to IR alone (Table 2). For example, we detected oxidation of isocitrate dehydrogenase [NAD] subunit α with IR alone, but we did not detect oxidation of this protein following IPC-IR. In contrast, only 50% of non-SNO proteins showed a significant reduction in oxidation. Taken together, these data suggest that IPC-induced protein SNO can protect from cysteine oxidation, and this occurs in part, through a direct block against oxidation.

IPC-Induced *S*-Nitrosylation of GAPDH Results in Faster Recovery of Activity During Reperfusion

We performed a set of experiments examining GAPDH activity in whole-heart homogenates subjected to the perfusion protocols shown in Figure 1B. GAPDH activity was largely inhibited with IPC and following IR (Figure 3A), and this is likely attributable to an increase in SNO (Figure 3B) and/or oxidation (Figure 3C). Both SNO and oxidation have been shown to inhibit GAPDH activity.[24,27] Interestingly, GAPDH activity levels returned to baseline with IPC-IR, as did SNO and oxidation levels, thus providing further evidence that IPC-induced protein SNO provides direct and transient protection against cysteine oxidation.

Discussion

Protein *S*-nitrosylation is known to increase following IPC,[2] and is thought to contribute to cardioprotection, in part, by reducing the oxidation of critical cysteine residues. This hypothesis is illustrated in Figure 1. It has been suggested that cysteine residues which are *S*-nitrosylated during cardioprotection are shielded from oxidation at the start of reperfusion.[18–20] Furthermore, it is well known that the burst of ROS generated during the first few minutes of reperfusion results in irreversible oxidation of many critical proteins. This hypothesis requires that *S*-nitrosylation be a transient modification; *S*-nitrosylation would need to be present on the cysteine residue at the start of reperfusion and during the initial burst of ROS (which is thought to last only a few minutes), but the *S*-nitrosylation would then need to degrade quickly after the burst of ROS so that normal protein function could resume. A rigorous test of this hypothesis requires a method for the measurement and identification of oxidation sites, as well as *S*-nitrosylation sites. Here, we describe a new method for measuring the oxidation sites of proteins in tandem with the measurement of *S*-nitrosylation. This Ox-RAC method was adapted from the recently published SNO-RAC method.[22] We also modified the SNO-RAC technique to accommodate the simultaneous measurement of oxidation and *S*-nitrosylation, thus allowing us to directly examine the hypothesis that *S*-nitrosylation shields cysteine residues from oxidation. Using this novel methodology, we have identified a large set of *S*-nitrosylated and oxidized proteins in our model of cardioprotection (Figure 2), and find that 76% of proteins showing an IPC-induced increase in *S*-nitrosylation, exhibit reduced or no oxidation at the same site following ischemia and early reperfusion (Table 2). Furthermore, the IPC-induced increase in protein *S*-nitrosylation is quickly reversed during early reperfusion (Figure 3). These results are consistent with the hypothesis that *S*-nitrosylation provides protection against cysteine oxidation during IR injury.

Nitroso-Redox Balance in Cardioprotection

IPC has been shown to reduce the burst of ROS that occurs during early reperfusion.[7] Consistent with this observation, we find that IPC reduced protein oxidation during early reperfusion (see Figure 2). Compared to IR alone, which is a condition in which the formation of ROS is favored,[21] there was a clear reduction in protein oxidation with IPC-IR. Interestingly, there were 17 proteins that were only oxidized with IR and these proteins might include irreversibly damaged proteins that contribute to dysfunction and cell death. Among the proteins oxidized with IR alone was a subunit of the mitochondrial import inner membrane translocase, Tim8B, and proteasome activator complex subunit 1. The mechanism through which IPC reduces protein oxidation is not well characterized, but is known to include a reduction in reperfusion ROS. NO has been shown to reduce reperfusion ROS, suggesting an important role for NO. Oxidant defense and/or oxidant repair mechanisms may also be activated with IPC. The reduction in reperfusion ROS is likely to be separate from the ability of *S*-nitrosylation to shield cysteine residues against ROS-induced oxidation. We hypothesize that NO, acting in part via *S*-nitrosylation, can also modify protein function during ischemia and early reperfusion and therefore play an additional role in protection. We have previously demonstrated that *S*-nitrosylation of the mitochondrial F_1F_0-ATPase dose dependently decreased activity.[2] This effect is consistent with the reduced ATP consumption observed in cardioprotective mechanisms.[28] IPC has also been proposed to signal through redox-sensitive mechanisms and antioxidants have been shown to block IPC-mediated protection.[6] Interestingly, IPC resulted in the oxidation of 13 unique proteins, including F-actin-capping protein subunit β, and

Table 2. Oxidation State of Peptides Showing a Significant Increase in Cysteine *S*-Nitrosylation With IPC As Identified via SNO-RAC/Ox-RAC Proteomic Analysis

Protein Name	Protein ID	Peptide Sequence	SNO or Ox Cys	SNO Ratio (IPC/Perfusion)	Ox Ratio (IR/IPC-IR)
Aconitate hydratase (M)	Q99KI0	VGLIGSCTNSSYEDMGR	385		1.69†
Aspartate aminotransferase	P05201	INMCGLTTK	391		Not detected in IR or IPC-IR
Aspartate aminotransferase (M)	P05202	VGAFTVVCK	295		1.41†
β-enolase	P21550	VNQIGSVTESIQACK	357		1.40†
Cysteine and glycine-rich protein 3	P50462	TVYHAEEIQCNGR	25		3.95†
Cysteine-rich protein 2	Q9DCT8	ASSVTTFTGEPNMCPR	126		1.70†
Cytochrome b-c1 complex subunit 1 (M)	Q9CZ13	VYEEDAVPGLTPCR	268		1.57
		LCTSATESEVTR	380	7.31*	0.67
Cytochrome c oxidase subunit 5B (M)	P19536	cPNCGTHYK	115		Not detected in IPC-IR
Electron transfer flavoprotein subunit α (M)	Q99LC5	TIYAGNALCTVK	155		1.55
Electron transfer flavoprotein subunit β (M)	Q9DCW4	EIIAVSCGPSQCQETIR	66, 71		1.60†
Enoyl-CoA hydratase (M)	Q8BH95	LVEEAIQCAEK	225		2.97†
Fructose-bisphosphate aldolase A	P05064	ALANSLACQGK	339	9.90*	2.04
Glyceraldehyde-3-phosphate	P16858	IVSNASCTTNCLAPLAK	150, 154	2.97*	2.74†
dehydrogenase		VPTPNVSVVDLTCR	245	2.10*	1.78†
Isocitrate dehydrogenase [NAD] subunit α (M)	Q9D6R2	IEAACFATIK	331		Not detected in IPC-IR
Isocitrate dehydrogenase [NADP] (M)	P54071	SSGGFVWACK	308		1.60
		VCVQTVESGAMTK	402	1.91	0.99
L-lactate dehydrogenase A chain	P06151	IVSSKDYCVTANSK	84		1.97
		VIGSGCNLDSAR	163	3.81*	2.16
Long-chain-fatty-acid-CoA ligase 1	P41216	GIQVSNNGPCLGSR	109		Not detected in IR or IPC-IR
Metallothionein-1	P02802	SCCSCCPVGCSK	33, 34, 36, 37, 41		Not detected in IR or IPC-IR
		GAADKCTCCA	57, 59, 60		Not detected in IR or IPC-IR
NADH dehydrogenase [ubiquinone] 1 α subcomplex subunit 10 (M)	Q99LC3	VITVDGNICSGK	67		1.69†
Peroxiredoxin-6	O08709	DFTPVCTTELGR	47		1.60†
Propionyl-CoA carboxylase α chain	Q91ZA3	MADEAVCVGPAPTSK	107		Not detected in IR or IPC-IR
Protein NipSnap homolog 2	O55126	ICQEVLPK	89	22.40*	Not detected in IR or IPC-IR
Succinate dehydrogenase [ubiquinone] flavoprotein (M)	Q8K2B3	VGSVLQEGCEK	536		Not detected in IR or IPC-IR
Succinyl-CoA ligase subunit β (M)	Q9Z2I9	ILACDDLDEAAK	430		1.58†
Triosephosphate isomerase	P17751	IAVAAQNCYK	67	3.40*	5.65†
		IIYGGSVTGATCK	218		4.12†
Tubulin β-4 chain	P04350	NMMAACDPR	303		5.74†
		TAVCDIPPR	354		1.54
Voltage-dependent anion channel protein 2 (M)	Q60930	SCSGVEFSTSGSSNTDTGK	48		2.72†

Each protein/peptide was identified from at least 3 of 5 SNO/Ox-RAC/LC-MS/MS proteomic analyses (peptides were filtered at a false discovery rate of 5%; peptides with ion scores <30 were not accepted). M indicates mitochondrial isoform; C, SNO cysteine residue; c, NEM-blocked cysteine residue. Peptides not detected under perfusion conditions contain a blank space in the ratio column. *$P<0.05$, perfusion vs IPC; †$P<0.05$, IR vs IPC-IR.

heat shock protein 60, which is an important mitochondrial chaperone protein. Furthermore, the fact that the proteins oxidized with IPC are quite dissimilar from those oxidized with IR alone and are quickly reversed with IPC-IR, may provide further evidence for redox-sensitive signaling.

Evaluation of the Ox-RAC Method

We report on a novel procedure for the measurement and site determination of protein cysteine oxidation. We identified 158 proteins with oxidative (non–*S*-nitrosylation) modifications at baseline. The majority of these proteins showed

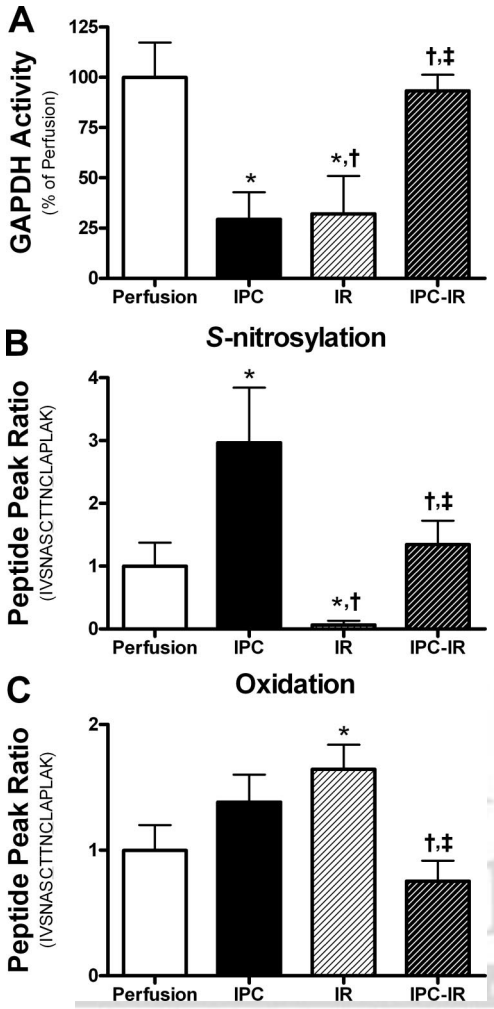

Figure 3. IPC-induced protein *S*-nitrosylation provides protection against cysteine oxidation. A, GAPDH activity shown as a percentage of perfusion (n=3 hearts/group). **B and C,** Representative peptide quantitative ratio as determined via label-free peptide analysis from SNO-RAC **(B)** and Ox-RAC **(C)** for GAPDH, demonstrating increased *S*-nitrosylation (SNO) and decreased oxidation (Ox) at the same cysteine residue (Cys150 and Cys154). Data are presented as means±SEM. **P*<0.05 vs perfusion; †*P*<0.05 vs IPC; ‡*P*<0.05 vs IR.

oxidative modification under all 4 conditions (Perfusion, IPC, IR, IPC-IR). These modifications include disulfide bonds, sulfenic acids, glutathiolation, and others. A number of methods have been described to measure redox sensitive cysteine residues.[26,29,30] Hurd et al used redox DIGE with a backward-labeling strategy and, on treatment of rat heart mitochondria with hydrogen peroxide, found 40 proteins with increased cysteine oxidation (this included *S*-nitrosylation as they did not pretreat with ascorbate).[26] The use of more physiological ROS generators (ie, antimycin treatment, stimulation of reverse electron transport) yielded only 6 oxidized proteins. Sites of oxidation were not identified with this method. Fu et al used isotope-coded affinity tag–labeling and DIGE with a forward labeling strategy to examine oxidized cysteine residues in extracts with and without hydrogen peroxide.[30] This method identified 63 proteins as targets of hydrogen peroxide; isotope-coded affinity tag identified 60 sites from 50 proteins. Thus, the Ox-RAC method compares favorably with published protocols. This technique allows for high-throughput identification of oxidized proteins and modification sites under biologically relevant conditions. As a result, this method promises to provide a new tool for further assessing the role of redox signaling in cardiovascular function.

Study Limitations

For the small percentage of peptides identified with the SNO-RAC protocol that have multiple *S*-nitrosylation sites, some of these cysteine residues may actually be sites of oxidative modification. This possibility exists because oxidative modifications, if present on resin-bound peptides, could be reduced by DTT during the elution step, thus leaving a free cysteine residue. SNO-RAC/Ox-RAC identifications from nonspecifically bound peptides are also possible. However, identifications from non–cysteine containing peptides accounted for approximately 6% of all peptide identifications for both the SNO-RAC and Ox-RAC protocols.

Summary

The nitroso-redox balance is crucial in the maintenance of normal myocardial function, and this balance can be critically affected by the widespread oxidation that occurs with IR injury. This newly developed SNO/Ox-RAC protocol provides the means to assess the nitroso-redox balance in the myocardium. When applied to a model of IPC, we determined that *S*-nitrosylation plays an important cardioprotective role by shielding cysteine residues from ROS-induced oxidation, thus maintaining the nitroso-redox balance.

Sources of Funding

This work was supported by NIH grants 1F32HL096142 (to M.K.) and 5R01HL039752 (to C.S.) and the National Heart, Lung, and Blood Institute/NIH Intramural Program (to A.A., E.M., G.W., J.S., and M.G.).

Disclosures

None.

References

1. Sun J, Picht E, Ginsburg KS, Bers DM, Steenbergen C, Murphy E. Hypercontractile female hearts exhibit increased S-nitrosylation of the L-type Ca2+ channel alpha1 subunit and reduced ischemia/reperfusion injury. *Circ Res*. 2006;98:403–411.
2. Sun J, Morgan M, Shen RF, Steenbergen C, Murphy E. Preconditioning results in S-nitrosylation of proteins involved in regulation of mitochondrial energetics and calcium transport. *Circ Res*. 2007;101:1155–1163.
3. Adachi T, Weisbrod RM, Pimentel DR, Ying J, Sharov VS, Schoneich C, Cohen RA. S-Glutathiolation by peroxynitrite activates SERCA during arterial relaxation by nitric oxide. *Nat Med*. 2004;10:1200–1207.
4. Wang H, Viatchenko-Karpinski S, Sun J, Gyorke I, Benkusky NA, Kohr MJ, Valdivia HH, Murphy E, Gyorke S, Ziolo MT. Regulation of myocyte contraction via neuronal nitric oxide synthase: role of ryanodine receptor S-nitrosylation. *J Physiol*. 2010;588:2905–2917.
5. Gonzalez DR, Beigi F, Treuer AV, Hare JM. Deficient ryanodine receptor S-nitrosylation increases sarcoplasmic reticulum calcium leak and arrhythmogenesis in cardiomyocytes. *Proc Natl Acad Sci U S A*. 2007;104:20612–20617.
6. Chen W, Gabel S, Steenbergen C, Murphy E. A redox-based mechanism for cardioprotection induced by ischemic preconditioning in perfused rat heart. *Circ Res*. 1995;77:424–429.

7. Vanden Hoek T, Becker LB, Shao ZH, Li CQ, Schumacker PT. Preconditioning in cardiomyocytes protects by attenuating oxidant stress at reperfusion. *Circ Res*. 2000;86:541–548.
8. Jones SP, Bolli R. The ubiquitous role of nitric oxide in cardioprotection. *J Mol Cell Cardiol*. 2006;40:16–23.
9. Costa AD, Garlid KD, West IC, Lincoln TM, Downey JM, Cohen MV, Critz SD. Protein kinase G transmits the cardioprotective signal from cytosol to mitochondria. *Circ Res*. 2005;97:329–336.
10. Lima B, Lam GK, Xie L, Diesen DL, Villamizar N, Nienaber J, Messina E, Bowles D, Kontos CD, Hare JM, Stamler JS, Rockman HA. Endogenous S-nitrosothiols protect against myocardial injury. *Proc Natl Acad Sci U S A*. 2009;106:6297–6302.
11. Burwell LS, Nadtochiy SM, Tompkins AJ, Young S, Brookes PS. Direct evidence for S-nitrosation of mitochondrial complex I. *Biochem J*. 2006; 394:627–634.
12. Handy DE, Loscalzo J. Nitric oxide and posttranslational modification of the vascular proteome: S-nitrosation of reactive thiols. *Arterioscler Thromb Vasc Biol*. 2006;26:1207–1214.
13. Hess DT, Matsumoto A, Kim SO, Marshall HE, Stamler JS. Protein S-nitrosylation: purview and parameters. *Nat Rev Mol Cell Biol*. 2005;6: 150–166.
14. Martinez-Ruiz A, Lamas S. S-nitrosylation: a potential new paradigm in signal transduction. *Cardiovasc Res*. 2004;62:43–52.
15. Sun J, Xin C, Eu JP, Stamler JS, Meissner G. Cysteine-3635 is responsible for skeletal muscle ryanodine receptor modulation by NO. *Proc Natl Acad Sci U S A*. 2001;98:11158–11162.
16. Tao L, Gao E, Bryan NS, Qu Y, Liu HR, Hu A, Christopher TA, Lopez BL, Yodoi J, Koch WJ, Feelisch M, Ma XL. Cardioprotective effects of thioredoxin in myocardial ischemia and reperfusion: role of S-nitrosation. *Proc Natl Acad Sci U S A*. 2004;101:11471–11476.
17. Chouchani ET, Hurd TR, Nadtochiy SM, Brookes PS, Fearnley IM, Lilley KS, Smith RA, Murphy MP. Identification of S-nitrosated mitochondrial proteins by S-nitrosothiol difference in gel electrophoresis (SNO-DIGE): implications for the regulation of mitochondrial function by reversible S-nitrosation. *Biochem J*. 2010;430:49–59.
18. Sun J, Steenbergen C, Murphy E. S-nitrosylation: NO-related redox signaling to protect against oxidative stress. *Antioxid Redox Signal*. 2006; 8:1693–1705.
19. Zimmet JM, Hare JM. Nitroso-redox interactions in the cardiovascular system. *Circulation*. 2006;114:1531–1544.
20. Sun J, Murphy E. Protein S-nitrosylation and cardioprotection. *Circ Res*. 2010;106:285–296.
21. Zweier JL, Talukder MA. The role of oxidants and free radicals in reperfusion injury. *Cardiovasc Res*. 2006;70:181–190.
22. Forrester MT, Thompson JW, Foster MW, Nogueira L, Moseley MA, Stamler JS. Proteomic analysis of S-nitrosylation and denitrosylation by resin-assisted capture. *Nat Biotechnol*. 2009;27:557–559.
23. Lin J, Steenbergen C, Murphy E, Sun J. Estrogen receptor-beta activation results in S-nitrosylation of proteins involved in cardioprotection. *Circulation*. 2009;120:245–254.
24. Padgett CM, Whorton AR. S-nitrosoglutathione reversibly inhibits GAPDH by S-nitrosylation. *Am J Physiol*. 1995;269:C739–C749.
25. Wang G, Wu WW, Zeng W, Chou CL, Shen RF. Label-free protein quantification using LC-coupled ion trap or FT mass spectrometry: reproducibility, linearity, and application with complex proteomes. *J Proteome Res*. 2006;5:1214–1223.
26. Hurd TR, Prime TA, Harbour ME, Lilley KS, Murphy MP. Detection of reactive oxygen species-sensitive thiol proteins by redox difference gel electrophoresis: implications for mitochondrial redox signaling. *J Biol Chem*. 2007;282:22040–22051.
27. Ishii T, Sunami O, Nakajima H, Nishio H, Takeuchi T, Hata F. Critical role of sulfenic acid formation of thiols in the inactivation of glyceraldehyde-3-phosphate dehydrogenase by nitric oxide. *Biochem Pharmacol*. 1999;58:133–143.
28. Murry CE, Jennings RB, Reimer KA. Preconditioning with ischemia: a delay of lethal cell injury in ischemic myocardium. *Circulation*. 1986; 74:1124–1136.
29. Wetzelberger K, Baba SP, Thirunavukkarasu M, Ho YS, Maulik N, Barski OA, Conklin DJ, Bhatnagar A. Postischemic deactivation of cardiac aldose reductase: role of glutathione S-transferase P and glutaredoxin in regeneration of reduced thiols from sulfenic acids. *J Biol Chem*. 285:26135–26148.
30. Fu C, Hu J, Liu T, Ago T, Sadoshima J, Li H. Quantitative analysis of redox-sensitive proteome with DIGE and ICAT. *J Proteome Res*. 2008;7:3789–3802.

Novelty and Significance

What Is Known?

- Ischemic preconditioning (IPC) is cardioprotective mechanism.
- S-Nitrosylation (SNO) is a reversible posttranslational modification that can alter the activity of target proteins.
- SNO is increased with myocardial IPC.
- SNO has been hypothesized to provide cardioprotection, in part, by shielding cysteine residues against oxidation.

What New Information Does This Article Contribute?

- A new method for the simultaneous, site-specific measurement of protein oxidation (Ox-RAC) and S-nitrosylation (SNO-RAC).
- Novel information in support of the hypothesis that SNO provides cardioprotective effects during ischemia/reperfusion (IR) injury by shielding specific cysteine residues against oxidation.

This study examined whether IPC-induced SNO exerts cardioprotective effects by directly shielding cysteine residues from oxidation. To test this hypothesis, we developed a novel method for simultaneous, site-specific measurement of protein oxidation and *S*-nitrosylation using resin-assisted capture. Using this methodology, we demonstrate that the total number of *S*-nitrosylated proteins is increased nearly 3-fold with myocardial IPC. Protein oxidation is also reduced with IPC. More specifically, for proteins that showed a significant increase in SNO with IPC, more than 75% showed a significant decrease or no oxidation following ischemia and early reperfusion at the same site when compared with IR alone. For non-SNO proteins, oxidation was reduced by only 50%. These results support the hypothesis that IPC-induced protein SNO provides cardioprotection by shielding cysteine residues from oxidation during IR injury. The method developed in this study may be useful for identifying redox-sensitive targets under other conditions associated with oxidative and nitrosative stress.

Circulation Research
JOURNAL OF THE AMERICAN HEART ASSOCIATION

Simultaneous Measurement of Protein Oxidation and *S*-Nitrosylation During Preconditioning and Ischemia/Reperfusion Injury With Resin-Assisted Capture

Mark J. Kohr, Junhui Sun, Angel Aponte, Guanghui Wang, Marjan Gucek, Elizabeth Murphy and Charles Steenbergen

Circ Res. published online December 30, 2010;
Circulation Research is published by the American Heart Association, 7272 Greenville Avenue, Dallas, TX 75231

Print ISSN: 0009-7330. Online ISSN: 1524-4571

SUPPLEMENTAL MATERIAL

Detailed Materials and Methods

Animals

Male C57BL/6 mice (n = 25) were obtained from Jackson Laboratories (Bar Harbor, ME). All animals utilized in this study were between the ages of 12-15 weeks. Prior to myocardial excision, mice were anesthetized with pentobarbital sodium (50-100 mg/kg) via intraperitoneal injection. This investigation conforms to the *Guide for the Care and Use of Laboratory Animals* published by the US National Institutes of Health (NIH publication No. 85-23, revised 1996) and was approved by the Institutional Laboratory Animal Care and Use Committee.

Solutions and drugs

Krebs-Henseleit buffer (KHB) consisted of (in mmol/L): NaCl (120), KCl (4.7), NaH_2PO_4 (1.2), $NaHCO_3$ (25), $MgSO_4$ (1.2), Glucose (10), and $CaCl_2$ (1.75); pH 7.4. KHB was bubbled with 95% O_2/5% CO_2. Ascorbate (Sigma, St. Louis, MO) was used as an *S*-nitrosylation (SNO)-specific reducing agent. Dithiothreitol (DTT; Pierce, Rockford, IL) was used as a general reducing agent. All solutions were made fresh on the day of experimentation.

Ischemia-Reperfusion treatment protocol

Hearts were Langendorff-perfused in the dark as previously described;[1, 2] treatment protocols are shown in Fig. 1a. Hearts were randomly subjected to a perfusion protocol (60 minute perfusion period), an IPC protocol (20 minute equilibration period, 4 cycles of 5 minutes ischemia and 5 minutes reperfusion), an IR protocol (60 minute equilibration period, 20 minute ischemic period, 5 minute reperfusion period), an IPC-IR protocol (20 minute equilibration period, 4 cycles of 5 minutes ischemia and 5 minutes reperfusion, 20 minute ischemic period, 5 minute reperfusion period), or an IPC-R protocol (20 minute equilibration period, 4 cycles of 5 minutes ischemia and 5 minutes reperfusion, 25 minute reperfusion period). Hearts were snap frozen in liquid nitrogen immediately following the treatment protocol.

Crude homogenate preparation

Crude heart homogenates were prepared as described previously.[1, 2] All subsequent procedures were performed in the dark. Hearts were powdered on liquid nitrogen with a mortar and pestle, and resuspended in 1.5 mL of homogenization buffer containing (in mmol/L): sucrose (300), HEPES-NaOH 7.7 (250), EDTA (1), and Neocuproine (0.1). An EDTA-free protease inhibitor tablet (Roche Diagnostics Corporation, Indianapolis, IN) was introduced just before use. Samples were then homogenized via Dounce glass homogenization on ice and centrifuged at 1,000 g for 2 minutes. The supernatant was recovered as total crude homogenate. Protein concentration was determined using the Bradford protein assay.

Oxidation site identification with resin-assisted capture

For oxidation site identification (Ox-RAC), samples (1 mg) were diluted in HEN buffer containing (in mmol/L): **H**EPES-NaOH 7.7 (250), **E**DTA (1), and **N**eocuproine (0.1) with 2.5% SDS and an EDTA-free protease inhibitor tablet (Roche Diagnostics Corporation). All buffers were de-gassed prior to use in order to prevent oxidation of the resin. Homogenates were then incubated with 20 mmol/L ascorbate for 45 minutes at room temperature in order to remove SNO. The inclusion of this step serves to distinguish SNO from other oxidative modifications; this step can be eliminated for the combined examination of SNO and other oxidative modifications. Samples were then incubated with 50 mmol/L *N*-ethylmaleimide (NEM; Sigma) for 20 minutes at 50^{o}C in order to block non-modified (i.e., free) and ascorbate-reduced thiol groups from modification; ascorbate and NEM were removed via acetone precipitation. Samples

were then resuspended in HENS and oxidized thiols were then reduced with 10 mmol/L DTT for 10 minutes at room temperature; DTT was removed via acetone precipitation. Samples were then resuspended in HEN with 1% SDS (HENS). Thiopropyl sepharose (GE Healthcare, Piscataway, NJ) was rehydrated for 25 minutes in DEPC H_2O. Following rehydration, 25 μL of the resin slurry was added to a Handee Mini Spin Column (Pierce) and washed with 5 x 0.5 mL DEPC H_2O, followed by 10 x 0.5 mL HEN buffer. Blocked samples were then added to the thiopropyl sepharose-containing spin column and rotated for 4 hours in the dark at room temperature. Proteins bind to the resin by forming disulfide linkages between reduced thiol groups of the protein and the thiol groups of the resin. Resin-bound proteins were then washed with 8 x 0.5 mL HENS buffer, followed by 4 x 0.5 mL HENS buffer diluted 1:10. Samples were then subjected to trypsin digestion (sequencing grade modified; Promega, Madison, WI) overnight at 37°C with rotation in buffer containing (in mmol/L): NH_4HCO_3 (50) and EDTA (1). Resin-bound peptides were then washed with 5 x 0.5 mL HENS buffer diluted 1:10, 5 x 0.5 mL 2 mol/L NaCl, 5 x 0.5 mL 80% acetonitrile/0.1% trifluoroacetic acid, and 5 x 0.5 mL HEN buffer diluted 1:10. Peptides were eluted for 30 minutes at room temperature in elution buffer containing (in mmol/L): DTT (20), NH_4CO_3 (10), and 50% methanol. The resin was then washed with an additional volume of elution buffer, followed by 2 volumes of DEPC water. All fractions were combined and concentrated via speedvac. Samples were then resuspended in 0.1% formic acid, and cleaned with a C_{18} column (ZipTip; Millipore, Billerica, MA). Liquid chromatography-tandem mass spectrometry (LC-MS/MS) was then performed using an LTQ Orbitrap XL mass spectrometer (Thermo Fisher Scientific, San Jose, CA) as described below. The MASCOT database search engine was used for protein identification as described below.

S-nitrosylation site identification with resin-assisted capture

A modified version of the SNO-RAC protocol was developed in order to examine protein SNO.[3] Samples (1 mg) were diluted in HEN buffer with 2.5% SDS and an EDTA-free protease inhibitor tablet (Roche Diagnostics Corporation). All buffers were de-gassed prior to use in order to prevent oxidation of the resin. Homogenates were then incubated with 50 mmol/L NEM for 20 minutes at 50°C in order to block non-modified (i.e., free) thiol groups from modification; NEM was removed via acetone precipitation. Samples were then resuspended in HENS. Thiopropyl sepharose resin (GE Healthcare, Piscataway, NJ) was rehydrated for 25 minutes in DEPC H_2O. Following rehydration, 25 μL of the resin slurry was added to a Handee Mini Spin Column (Pierce) and washed with 5 x 0.5 mL DEPC H_2O, followed by 10 x 0.5 mL HEN buffer. Blocked samples were then added to the thiopropyl sepharose-containing spin column, along with 20 mmol/L ascorbate to reduce SNO, and rotated for four hours in the dark at room temperature. Proteins bind to the resin by forming disulfide linkages between reduced thiol groups of the protein and the thiol groups of the resin. Resin-bound proteins were then washed with 8 x 0.5 mL HENS buffer, followed by 4 x 0.5 mL HENS buffer diluted 1:10. Samples were then subjected to trypsin digestion (sequencing grade modified; Promega) overnight at 37°C with rotation in buffer containing (in mmol/L): NH_4HCO_3 (50) and EDTA (1). Resin-bound peptides were then washed with 5 x 0.5 mL HENS buffer diluted 1:10, 5 x 0.5 mL 2 mol/L NaCl, 5 x 0.5 mL 80% acetonitrile (v/v)/0.1% trifluoroacetic acid (v/v), and 5 x 0.5 mL HEN buffer diluted 1:10. Peptides were eluted for 30 minutes at room temperature in elution buffer containing (in mmol/L): DTT (20), NH_4HCO_3 (10), and 50% methanol (v/v). The resin was then washed with an additional volume of elution buffer, followed by 2 volumes of DEPC water. All fractions were combined and concentrated via speedvac. Samples were then resuspended in 0.1% formic acid, and cleaned with a C_{18} column (ZipTip; Millipore). LC-MS/MS was then performed using an LTQ Orbitrap XL mass spectrometer (Thermo Fisher Scientific) as described below. The MASCOT database search engine was used for protein identification as described below.

Liquid chromatography-tandem mass spectrometry analysis on LTQ Orbitrap XL

LC-MS/MS was performed using an Eksigent nano-LC 1D plus system (Dublin, CA) coupled to an LTQ Orbitrap XL mass spectrometer (Thermo Fisher Scientific) using CID fragmentation. Peptides were first loaded onto a Zorbax 300SB-C_{18} trap column (Agilent, Palo Alto, CA) at a flow rate of 5 µL/minute for 10 minutes, and then separated on a reversed-phase PicoFrit analytical column (New Objective, Woburn, MA) using a 40-minute linear gradient of 2-40% acetonitrile in 0.1% formic acid at a flow rate of 300 nL/minute. LTQ Orbitrap XL settings were as follows: spray voltage 1.5 kV, and full MS mass range: m/z 200 to 2000. The LTQ Orbitrap XL was operated in a data-dependent mode (i.e., one MS1 high resolution [30,000] scan for precursor ions followed by six data-dependent MS2 scans for precursor ions above a threshold ion count of 2000 with collision energy of 35%).

MASCOT Database Search

The raw file generated from the LTQ Orbitrap XL was analyzed using Proteome Discoverer v1.1 software (Thermo Fisher Scientific) with the NIH six-processor MASCOT cluster search engine (http://biospec.nih.gov, version 2.3). The following search criteria were used: database, Swiss-Prot (Swiss Institute of Bioinformatics); taxonomy, Mus musculus (mouse); enzyme, trypsin; miscleavages, 3; variable modifications, oxidation (M), *N*-methylmaleimide (C), deamidation (NQ); MS peptide tolerance 25 ppm; MS/MS tolerance as 0.8 Da. All peptides were assigned an ion score. The ion score is a measure of how well the MS/MS spectra matches the stated peptide; higher scores represent more confident matches. Ion scores were generated as $-10*LOG_{10}(P)$, where P represents the probability that the match is random. For a more detailed explanation of the ion score, please see the following reference.[4] Peptides with ion scores below 30 were not accepted. Peptides were filtered at a false discovery rate (FDR) of 5%, as determined by a targeted decoy database search with a significance threshold of 0.03. Identifications from non-specifically bound peptides (i.e., non-cysteine containing peptides) accounted for approximately 6% of all peptide identifications for both the SNO-RAC and Ox-RAC protocols; non-cysteine containing peptides were filtered from the data set.

Label-free peptide quantification and analysis

Relative quantification of SNO and oxidation was performed using QUOIL (**QU**antification with**O**ut **I**sotope **L**abeling), an in-house software program designed as a label-free approach to peptide quantification by LC-MS/MS.[5] This label-free approach relies on the direct comparison of peptide area-under-the-curve peaks from each LC-MS/MS run. More specifically, a peptide's chromatogram peak in each LC-MS/MS run was reconstructed based on its precursor m/z value. Quantitative ratios were then obtained by normalizing the peptide peak areas against a chosen reference (i.e., perfusion control for common peptides). The resulting ratios reflect the relative quantity of a peptide (and hence the corresponding SNO or oxidation level) in different samples, but the absolute amounts of the protein SNO and oxidation cannot be determined, since unmodified protein does not bind to the column and was not measured.

Glyceraldehyde-3-phosphate dehydrogenase activity assay

GAPDH activity was measured as described previously.[6] The assay buffer consisted of (in mmol/L): sodium pyrophosphate (10), sodium arsenate (25), NAD^+ (0.25); pH 8.5. Whole heart homogenate (10 µg) was diluted in 100 µL of assay buffer and the activity of GAPDH was monitored by following the reduction of NAD^+ to NADH at 340 nm using a FLUOstar Omega plate reader (BMG Labtech, Offenburg, Germany). The assay was initiated upon the addition of 0.5 mmol/L glyceraldehyde-3-phosphate (Sigma).

Statistics

Statistical significance ($p<0.05$) was determined between groups using an ANOVA for multiple groups or a Student's *t*-test for two groups.

Online Table I. **Selected peptides showing cysteine oxidation as identified via Ox-RAC proteomic analysis.**

Protein Name	Protein ID	Peptide Sequence	Ox Cys	Perfusion		IPC		IR		IPC-IR	
				Ratio	Ion Score	Ratio	Ion Score	Ratio	Ion Score	Ratio	Ion Score
Citrate synthase (M)	Q9CZU6	GYSIPEC<u>C</u>QK	101								
Cytochrome b-c1 complex subunit 1 (M)	Q9CZ13	VYEEDAVPGLTP<u>C</u>R	268	1	81	1.25	101	0.93	84	1.24	94
		L<u>C</u>TSATESEVTR	380	1	95	0.23	93	0.50	93	0.50	95
Fructose-bisphosphate aldolase A	P05064	ALANSLA<u>C</u>QGK	339	1	83	1.13	86	$1.85^{\dagger,*}$	80	0.32	67
Glyceraldehyde-3-phosphate dehydrogenase	P16858	IVSNAS<u>C</u>TTN<u>C</u>LAPLAK	150,154	1	124	1.38	138	1.65^{*}	122	$0.75^{\dagger,\ddagger}$	122
		VPTPNVSVVDLT<u>C</u>R	245	1	100	3.25^{*}	100	3.79^{*}	101	$1.83^{\dagger,\ddagger}$	102
Isocitrate dehydrogenase [NADP] (M)	P54071	SSGGFVWA<u>C</u>K	308	1	77	1.34	76	1.28	83	1.01	63
		V<u>C</u>VQTVESGAMTK	402	1	110	17.88^{*}	112	$41.33^{*,\dagger}$	106	$7.93^{*,\dagger}$	107
L-lactate dehydrogenase A chain	P06151	IVSSKDY<u>C</u>VTANSK	84	1	93	2.05	85	2.79^{*}	89	$0.33^{*,\dagger}$	87
		VIGSG<u>C</u>NLDSAR	163	1	103	5.46^{*}	95	$0.89^{\dagger}$	99	$0.80^{\dagger}$	106
Malate dehydrogenase	P14152	VIVVGNPANTN<u>C</u>LTASK	137	1	89	1.97^{*}	89	1.62	88	$1.05^{\dagger}$	81
Malate dehydrogenase (M)	P08249	EGVVE<u>C</u>SFVQSK	275	1	84	2.22^{*}	72	3.33^{*}	76	2.35^{*}	75
Protein NipSnap homolog 2	O55126	I<u>C</u>QEVLPK	89								
Succinyl-CoA ligase α (M)	Q9WUM5	II<u>C</u>QGFTGK	60				47		55		48
Triosephosphate isomerase	P17751	IAVAAQN<u>C</u>YK	67	1	40	1.61	48	1.81^{*}	46	$0.68^{*,\dagger,\ddagger}$	42
		IIYGGSVTGAT<u>C</u>K	218	1	103	2.88^{*}	103	2.33^{*}	98	$1.04^{\dagger,\ddagger}$	90
Aconitate hydratase (M)	Q99KI0	VGLIGS<u>C</u>TNSSYEDMGR	385	1	132	2.88	128	2.03^{*}	137	$0.95^{\ddagger}$	128
Aspartate aminotransferase	P05201	INM<u>C</u>GLTTK	391								
Aspartate aminotransferase (M)	P05202	VGAFTVV<u>C</u>K	295	1	95	1.29^{*}	99	1.70^{*}	97	$1.30^{*,\ddagger}$	115
β-enolase	P21550	VNQIGSVTESIQA<u>C</u>K	357	1	128	1.35^{*}	115	1.71^{*}	123	$0.69^{*,\dagger,\ddagger}$	123
Cysteine and glycine-rich protein 3	P50462	TVYHAEEIQ<u>C</u>NGR	25	1	72	2.49	84	1.61^{*}	73	$0.61^{*,\ddagger}$	87
Cysteine-rich protein 2	Q9DCT8	ASSVTTFTGEPNM<u>C</u>PR	126	1	89	2.27^{*}	90	1.74^{*}	88	$1.04^{\dagger,\ddagger}$	98
Cytochrome c oxidase subunit 5b (M)	P19536	cPN<u>C</u>GTHYK	115						33		
Electron transfer flavoprotein subunit α (M)	Q99LC5	TIYAGNAL<u>C</u>TVK	155	1	63	2.38	108	3.87	67	0.96	65
Electron transfer flavoprotein subunit β (M)	Q9DCW4	EIIAVS<u>C</u>GPSQ<u>C</u>QETIR	66,71	1	124	1.01	107	1.42^{*}	127	$0.44^{\ddagger}$	128
Enoyl-CoA hydratase (M)	Q8BH95	LVEEAIQ<u>C</u>AEK	225	1	88	6.06^{*}	92	7.28^{*}	86	$2.24^{\dagger,\ddagger}$	78
Isocitrate dehydrogenase [NAD] subunit α (M)	Q9D6R2	IEAA<u>C</u>FATIK	331				56		57		
Long-chain-fatty-acid-CoA ligase 1	P41216	GIQVSNNGP<u>C</u>LGSR	109								
Metallothionein-1	P02802	S<u>CC</u>S<u>CC</u>PVG<u>C</u>SK	33,34,36 37,41								
		GAADK<u>C</u>T<u>CC</u>A	57,59,60								
NADH dehydrogenase [ubiquinone] 1 α subcomplex subunit 10 (M)	Q99LC3	VITVDGNI<u>C</u>SGK	67	1	61	1.31	67	1.45^{*}	70	$1.30^{\ddagger}$	68
Peroxiredoxin-6	O08709	DFTPV<u>C</u>TTELGR	47	1	67	8.47^{*}	71	9.17^{*}	65	$5.11^{*,\dagger,\ddagger}$	65
Propionyl-CoA carboxylase α chain	Q91ZA3	MADEAV<u>C</u>VGPAPTSK	107								
Succinate dehydrogenase [ubiquinone] flavoprotein (M)	**Q8K2B3**	VGSVLQEG<u>C</u>EK	536								
Succinyl-CoA ligase subunit β (M)	Q9Z2I9	ILA<u>C</u>DDLDEAAK	430	1	75	4.50^{*}	69	5.38^{*}	77	$1.71^{*,\dagger,\ddagger}$	75
Sarcoplasmic/endoplasmic reticulum calcium ATPase 2	O55143	SMSVY<u>C</u>TPNKPSR	498	1	57	2.98	65	1.36	55	1.31	59
Tubulin β-4 chain	**P04350**	NMMAA<u>C</u>DPR	303	1	62	3.28^{*}	59	1.60^{*}	64	$0.36^{*,\dagger,\ddagger}$	62
		TAV<u>C</u>DIPPR	354	1	53			2.05^{*}	52	$1.35^{\ddagger}$	52
Very long-chain specific acyl-CoA dehydrogenase (M)	P50544	SSAIPSP<u>C</u>GK	238	1	35	4.00^{*}	42	$1.17^{\dagger}$	39	$0.39^{*,\dagger}$	40
Voltage-dependent anion channel protein 2 (M)	Q60930	S<u>C</u>SGVEFSTSGSSNTDTGK	48	1	122	3.24^{*}	127	$2.11^{*,\dagger}$	131	$1.50^{\dagger,\ddagger}$	137

Proteins selected for inclusion in Online Table I are the same proteins from Table 1. Each protein/peptide was identified from at least three of five SNO-RAC/LC-MS/MS proteomic analyses (peptides were filtered at a false discovery rate of 5%; peptides with ion scores below 30 were not accepted). (M): mitochondrial isoform; (<u>C</u>): SNO cysteine residue; (c): NEM-blocked cysteine residue; Peptides not detected under the specified condition contain a blank space in the ion score column. Peptide quantitative ratio was determined via label-free peptide analysis. $^{*}p<0.05$ vs. Perfusion; $^{\dagger}p<0.05$ vs. IPC; $^{\ddagger}p<0.05$ vs. IR.

Additional Online Table Legends

Online Table II. **Oxidized protein/peptide identifications from perfusion hearts as identified via Ox-RAC proteomic analysis.** LC-MS/MS derived peptide sequences and MASCOT MS2 search identifications (false discovery rate of 5%). Peptide identifications with ions scores below 30 were not accepted; non-cysteine containing peptides were filtered from the data set. To view peptide sequences, click on the '+' symbol found on the left side of the spreadsheet. Each of 5 biological replicates was run in order to increase protein/peptide identifications; replicates are identified in column headings as A2 (Perfusion Heart 1), B2 (Perfusion Heart 2), C2 (Perfusion Heart 3), D2 (Perfusion Heart 4), and E2 (Perfusion Heart 5). Please note that Online Table II includes all Ox-RAC protein/peptide identifications from perfusion hearts, including those observed in fewer than three of five Ox-RAC proteomic analyses.

Online Table III. **Oxidized protein/peptide identifications from IR hearts as identified via Ox-RAC proteomic analysis.** LC-MS/MS derived peptide sequences and MASCOT MS2 search identifications (false discovery rate of 5%). Peptide identifications with ions scores below 30 were not accepted; non-cysteine containing peptides were filtered from the data set. To view peptide sequences, click on the '+' symbol found on the left side of the spreadsheet. Each of 5 biological replicates was run in order to increase protein/peptide identifications; replicates are identified in column headings as A2 (IR Heart 1), B2 (IR Heart 2), C2 (IR Heart 3), D2 (IR Heart 4), and E2 (IR Heart 5). Please note that Online Table III includes all Ox-RAC protein/peptide identifications from IR hearts, including those observed in fewer than three of five Ox-RAC proteomic analyses.

Online Table IV. **Oxidized protein/peptide identifications from IPC hearts as identified via Ox-RAC proteomic analysis.** LC-MS/MS derived peptide sequences and MASCOT MS2 search identifications (false discovery rate of 5%). Peptide identifications with ions scores below 30 were not accepted; non-cysteine containing peptides were filtered from the data set. To view peptide sequences, click on the '+' symbol found on the left side of the spreadsheet. Each of 5 biological replicates was run in order to increase protein/peptide identifications; replicates are identified in column headings as A2 (IPC Heart 1), B2 (IPC Heart 2), C2 (IPC Heart 3), D2 (IPC Heart 4), and E2 (IPC Heart 5). Please note that Online Table IV includes all Ox-RAC protein/peptide identifications from IPC hearts, including those observed in fewer than three of five Ox-RAC proteomic analyses.

Online Table V. **Oxidized protein/peptide identifications from IPC-IR hearts as identified via Ox-RAC proteomic analysis.** LC-MS/MS derived peptide sequences and MASCOT MS2 search identifications (false discovery rate of 5%). Peptide identifications with ions scores below 30 were not accepted; non-cysteine containing peptides were filtered from the data set. To view peptide sequences, click on the '+' symbol found on the left side of the spreadsheet. Each of 5 biological replicates was run in order to increase protein/peptide identifications; replicates are identified in column headings as A2 (IPC-IR Heart 1), B2 (IPC-IR Heart 2), C2 (IPC-IR Heart 3), D2 (IPC-IR Heart 4), and E2 (IPC-IR Heart 5). Please note that Online Table V includes all Ox-RAC protein/peptide identifications from IPC-IR hearts, including those observed in fewer than three of five Ox-RAC proteomic analyses.

Supplemental References

1. Lin J, Steenbergen C, Murphy E, Sun J. Estrogen receptor-beta activation results in S-nitrosylation of proteins involved in cardioprotection. *Circulation.* 2009;120:245-254.

2. Sun J, Morgan M, Shen RF, Steenbergen C, Murphy E. Preconditioning results in S-nitrosylation of proteins involved in regulation of mitochondrial energetics and calcium transport. *Circ Res.* 2007;101:1155-1163.

3. Forrester MT, Thompson JW, Foster MW, Nogueira L, Moseley MA, Stamler JS. Proteomic analysis of S-nitrosylation and denitrosylation by resin-assisted capture. *Nat Biotechnol.* 2009;27:557-559.

4. Perkins DN, Pappin DJ, Creasy DM, Cottrell JS. Probability-based protein identification by searching sequence databases using mass spectrometry data. *Electrophoresis.* 1999;20:3551-3567.

5. Wang G, Wu WW, Zeng W, Chou CL, Shen RF. Label-free protein quantification using LC-coupled ion trap or FT mass spectrometry: Reproducibility, linearity, and application with complex proteomes. *J Proteome Res.* 2006;5:1214-1223.

6. Padgett CM, Whorton AR. S-nitrosoglutathione reversibly inhibits GAPDH by S-nitrosylation. *Am J Physiol.* 1995;269:C739-C749.

SUPPLEMENTAL MATERIAL

Detailed Materials and Methods

Animals

Male C57BL/6 mice (n = 25) were obtained from Jackson Laboratories (Bar Harbor, ME). All animals utilized in this study were between the ages of 12-15 weeks. Prior to myocardial excision, mice were anesthetized with pentobarbital sodium (50-100 mg/kg) via intraperitoneal injection. This investigation conforms to the *Guide for the Care and Use of Laboratory Animals* published by the US National Institutes of Health (NIH publication No. 85-23, revised 1996) and was approved by the Institutional Laboratory Animal Care and Use Committee.

Solutions and drugs

Krebs-Henseleit buffer (KHB) consisted of (in mmol/L): NaCl (120), KCl (4.7), NaH_2PO_4 (1.2), $NaHCO_3$ (25), $MgSO_4$ (1.2), Glucose (10), and $CaCl_2$ (1.75); pH 7.4. KHB was bubbled with 95% O_2/5% CO_2. Ascorbate (Sigma, St. Louis, MO) was used as an *S*-nitrosylation (SNO)-specific reducing agent. Dithiothreitol (DTT; Pierce, Rockford, IL) was used as a general reducing agent. All solutions were made fresh on the day of experimentation.

Ischemia-Reperfusion treatment protocol

Hearts were Langendorff-perfused in the dark as previously described;[1, 2] treatment protocols are shown in Fig. 1a. Hearts were randomly subjected to a perfusion protocol (60 minute perfusion period), an IPC protocol (20 minute equilibration period, 4 cycles of 5 minutes ischemia and 5 minutes reperfusion), an IR protocol (60 minute equilibration period, 20 minute ischemic period, 5 minute reperfusion period), an IPC-IR protocol (20 minute equilibration period, 4 cycles of 5 minutes ischemia and 5 minutes reperfusion, 20 minute ischemic period, 5 minute reperfusion period), or an IPC-R protocol (20 minute equilibration period, 4 cycles of 5 minutes ischemia and 5 minutes reperfusion, 25 minute reperfusion period). Hearts were snap frozen in liquid nitrogen immediately following the treatment protocol.

Crude homogenate preparation

Crude heart homogenates were prepared as described previously.[1, 2] All subsequent procedures were performed in the dark. Hearts were powdered on liquid nitrogen with a mortar and pestle, and resuspended in 1.5 mL of homogenization buffer containing (in mmol/L): sucrose (300), HEPES-NaOH 7.7 (250), EDTA (1), and Neocuproine (0.1). An EDTA-free protease inhibitor tablet (Roche Diagnostics Corporation, Indianapolis, IN) was introduced just before use. Samples were then homogenized via Dounce glass homogenization on ice and centrifuged at 1,000 g for 2 minutes. The supernatant was recovered as total crude homogenate. Protein concentration was determined using the Bradford protein assay.

Oxidation site identification with resin-assisted capture

For oxidation site identification (Ox-RAC), samples (1 mg) were diluted in HEN buffer containing (in mmol/L): **H**EPES-NaOH 7.7 (250), **E**DTA (1), and **N**eocuproine (0.1) with 2.5% SDS and an EDTA-free protease inhibitor tablet (Roche Diagnostics Corporation). All buffers were de-gassed prior to use in order to prevent oxidation of the resin. Homogenates were then incubated with 20 mmol/L ascorbate for 45 minutes at room temperature in order to remove SNO. The inclusion of this step serves to distinguish SNO from other oxidative modifications; this step can be eliminated for the combined examination of SNO and other oxidative modifications. Samples were then incubated with 50 mmol/L *N*-ethylmaleimide (NEM; Sigma) for 20 minutes at 50^{o}C in order to block non-modified (i.e., free) and ascorbate-reduced thiol groups from modification; ascorbate and NEM were removed via acetone precipitation. Samples

were then resuspended in HENS and oxidized thiols were then reduced with 10 mmol/L DTT for 10 minutes at room temperature; DTT was removed via acetone precipitation. Samples were then resuspended in HEN with 1% SDS (HENS). Thiopropyl sepharose (GE Healthcare, Piscataway, NJ) was rehydrated for 25 minutes in DEPC H_2O. Following rehydration, 25 μL of the resin slurry was added to a Handee Mini Spin Column (Pierce) and washed with 5 x 0.5 mL DEPC H_2O, followed by 10 x 0.5 mL HEN buffer. Blocked samples were then added to the thiopropyl sepharose-containing spin column and rotated for 4 hours in the dark at room temperature. Proteins bind to the resin by forming disulfide linkages between reduced thiol groups of the protein and the thiol groups of the resin. Resin-bound proteins were then washed with 8 x 0.5 mL HENS buffer, followed by 4 x 0.5 mL HENS buffer diluted 1:10. Samples were then subjected to trypsin digestion (sequencing grade modified; Promega, Madison, WI) overnight at 37°C with rotation in buffer containing (in mmol/L): NH_4HCO_3 (50) and EDTA (1). Resin-bound peptides were then washed with 5 x 0.5 mL HENS buffer diluted 1:10, 5 x 0.5 mL 2 mol/L NaCl, 5 x 0.5 mL 80% acetonitrile/0.1% trifluoroacetic acid, and 5 x 0.5 mL HEN buffer diluted 1:10. Peptides were eluted for 30 minutes at room temperature in elution buffer containing (in mmol/L): DTT (20), NH_4CO_3 (10), and 50% methanol. The resin was then washed with an additional volume of elution buffer, followed by 2 volumes of DEPC water. All fractions were combined and concentrated via speedvac. Samples were then resuspended in 0.1% formic acid, and cleaned with a C_{18} column (ZipTip; Millipore, Billerica, MA). Liquid chromatography-tandem mass spectrometry (LC-MS/MS) was then performed using an LTQ Orbitrap XL mass spectrometer (Thermo Fisher Scientific, San Jose, CA) as described below. The MASCOT database search engine was used for protein identification as described below.

S-nitrosylation site identification with resin-assisted capture

A modified version of the SNO-RAC protocol was developed in order to examine protein SNO.[3] Samples (1 mg) were diluted in HEN buffer with 2.5% SDS and an EDTA-free protease inhibitor tablet (Roche Diagnostics Corporation). All buffers were de-gassed prior to use in order to prevent oxidation of the resin. Homogenates were then incubated with 50 mmol/L NEM for 20 minutes at 50°C in order to block non-modified (i.e., free) thiol groups from modification; NEM was removed via acetone precipitation. Samples were then resuspended in HENS. Thiopropyl sepharose resin (GE Healthcare, Piscataway, NJ) was rehydrated for 25 minutes in DEPC H_2O. Following rehydration, 25 μL of the resin slurry was added to a Handee Mini Spin Column (Pierce) and washed with 5 x 0.5 mL DEPC H_2O, followed by 10 x 0.5 mL HEN buffer. Blocked samples were then added to the thiopropyl sepharose-containing spin column, along with 20 mmol/L ascorbate to reduce SNO, and rotated for four hours in the dark at room temperature. Proteins bind to the resin by forming disulfide linkages between reduced thiol groups of the protein and the thiol groups of the resin. Resin-bound proteins were then washed with 8 x 0.5 mL HENS buffer, followed by 4 x 0.5 mL HENS buffer diluted 1:10. Samples were then subjected to trypsin digestion (sequencing grade modified; Promega) overnight at 37°C with rotation in buffer containing (in mmol/L): NH_4HCO_3 (50) and EDTA (1). Resin-bound peptides were then washed with 5 x 0.5 mL HENS buffer diluted 1:10, 5 x 0.5 mL 2 mol/L NaCl, 5 x 0.5 mL 80% acetonitrile (v/v)/0.1% trifluoroacetic acid (v/v), and 5 x 0.5 mL HEN buffer diluted 1:10. Peptides were eluted for 30 minutes at room temperature in elution buffer containing (in mmol/L): DTT (20), NH_4HCO_3 (10), and 50% methanol (v/v). The resin was then washed with an additional volume of elution buffer, followed by 2 volumes of DEPC water. All fractions were combined and concentrated via speedvac. Samples were then resuspended in 0.1% formic acid, and cleaned with a C_{18} column (ZipTip; Millipore). LC-MS/MS was then performed using an LTQ Orbitrap XL mass spectrometer (Thermo Fisher Scientific) as described below. The MASCOT database search engine was used for protein identification as described below.

Liquid chromatography-tandem mass spectrometry analysis on LTQ Orbitrap XL

LC-MS/MS was performed using an Eksigent nano-LC 1D plus system (Dublin, CA) coupled to an LTQ Orbitrap XL mass spectrometer (Thermo Fisher Scientific) using CID fragmentation. Peptides were first loaded onto a Zorbax 300SB-C_{18} trap column (Agilent, Palo Alto, CA) at a flow rate of 5 µL/minute for 10 minutes, and then separated on a reversed-phase PicoFrit analytical column (New Objective, Woburn, MA) using a 40-minute linear gradient of 2-40% acetonitrile in 0.1% formic acid at a flow rate of 300 nL/minute. LTQ Orbitrap XL settings were as follows: spray voltage 1.5 kV, and full MS mass range: m/z 200 to 2000. The LTQ Orbitrap XL was operated in a data-dependent mode (i.e., one MS1 high resolution [30,000] scan for precursor ions followed by six data-dependent MS2 scans for precursor ions above a threshold ion count of 2000 with collision energy of 35%).

MASCOT Database Search

The raw file generated from the LTQ Orbitrap XL was analyzed using Proteome Discoverer v1.1 software (Thermo Fisher Scientific) with the NIH six-processor MASCOT cluster search engine (http://biospec.nih.gov, version 2.3). The following search criteria were used: database, Swiss-Prot (Swiss Institute of Bioinformatics); taxonomy, Mus musculus (mouse); enzyme, trypsin; miscleavages, 3; variable modifications, oxidation (M), *N*-methylmaleimide (C), deamidation (NQ); MS peptide tolerance 25 ppm; MS/MS tolerance as 0.8 Da. All peptides were assigned an ion score. The ion score is a measure of how well the MS/MS spectra matches the stated peptide; higher scores represent more confident matches. Ion scores were generated as $-10*LOG_{10}(P)$, where P represents the probability that the match is random. For a more detailed explanation of the ion score, please see the following reference.[4] Peptides with ion scores below 30 were not accepted. Peptides were filtered at a false discovery rate (FDR) of 5%, as determined by a targeted decoy database search with a significance threshold of 0.03. Identifications from non-specifically bound peptides (i.e., non-cysteine containing peptides) accounted for approximately 6% of all peptide identifications for both the SNO-RAC and Ox-RAC protocols; non-cysteine containing peptides were filtered from the data set.

Label-free peptide quantification and analysis

Relative quantification of SNO and oxidation was performed using QUOIL (**QU**antification with**O**ut **I**sotope **L**abeling), an in-house software program designed as a label-free approach to peptide quantification by LC-MS/MS.[5] This label-free approach relies on the direct comparison of peptide area-under-the-curve peaks from each LC-MS/MS run. More specifically, a peptide's chromatogram peak in each LC-MS/MS run was reconstructed based on its precursor m/z value. Quantitative ratios were then obtained by normalizing the peptide peak areas against a chosen reference (i.e., perfusion control for common peptides). The resulting ratios reflect the relative quantity of a peptide (and hence the corresponding SNO or oxidation level) in different samples, but the absolute amounts of the protein SNO and oxidation cannot be determined, since unmodified protein does not bind to the column and was not measured.

Glyceraldehyde-3-phosphate dehydrogenase activity assay

GAPDH activity was measured as described previously.[6] The assay buffer consisted of (in mmol/L): sodium pyrophosphate (10), sodium arsenate (25), NAD^+ (0.25); pH 8.5. Whole heart homogenate (10 µg) was diluted in 100 µL of assay buffer and the activity of GAPDH was monitored by following the reduction of NAD^+ to NADH at 340 nm using a FLUOstar Omega plate reader (BMG Labtech, Offenburg, Germany). The assay was initiated upon the addition of 0.5 mmol/L glyceraldehyde-3-phosphate (Sigma).

Statistics

Statistical significance ($p<0.05$) was determined between groups using an ANOVA for multiple groups or a Student's *t*-test for two groups.

Online Table I. **Selected peptides showing cysteine oxidation as identified via Ox-RAC proteomic analysis.**

Protein Name	Protein ID	Peptide Sequence	Ox Cys	Perfusion		IPC		IR		IPC-IR	
				Ratio	Ion Score	Ratio	Ion Score	Ratio	Ion Score	Ratio	Ion Score
Citrate synthase (M)	Q9CZU6	GYSIPEC<u>C</u>QK	101								
Cytochrome b-c1 complex subunit 1 (M)	Q9CZ13	VYEEDAVPGLTP<u>C</u>R	268	1	81	1.25	101	0.93	84	1.24	94
		L<u>C</u>TSATESEVTR	380	1	95	0.23	93	0.50	93	0.50	95
Fructose-bisphosphate aldolase A	P05064	ALANSLA<u>C</u>QGK	339	1	83	1.13	86	$1.85^{\dagger,*}$	80	0.32	67
Glyceraldehyde-3-phosphate dehydrogenase	P16858	IVSNAS<u>C</u>TTN<u>C</u>LAPLAK	150,154	1	124	1.38	138	1.65^{*}	122	$0.75^{\dagger,\ddagger}$	122
		VPTPNVSVVDLT<u>C</u>R	245	1	100	3.25^{*}	100	3.79^{*}	101	$1.83^{\dagger,\ddagger}$	102
Isocitrate dehydrogenase [NADP] (M)	P54071	SSGGFVWA<u>C</u>K	308	1	77	1.34	76	1.28	83	1.01	63
		V<u>C</u>VQTVESGAMTK	402	1	110	17.88^{*}	112	$41.33^{*,\dagger}$	106	$7.93^{*,\dagger}$	107
L-lactate dehydrogenase A chain	P06151	IVSSKDY<u>C</u>VTANSK	84	1	93	2.05	85	2.79^{*}	89	$0.33^{*,\dagger}$	87
		VIGSG<u>C</u>NLDSAR	163	1	103	5.46^{*}	95	$0.89^{\dagger}$	99	$0.80^{\dagger}$	106
Malate dehydrogenase	P14152	VIVVGNPANTN<u>C</u>LTASK	137	1	89	1.97^{*}	89	1.62	88	$1.05^{\dagger}$	81
Malate dehydrogenase (M)	P08249	EGVVE<u>C</u>SFVQSK	275	1	84	2.22^{*}	72	3.33^{*}	76	2.35^{*}	75
Protein NipSnap homolog 2	O55126	I<u>C</u>QEVLPK	89								
Succinyl-CoA ligase α (M)	Q9WUM5	II<u>C</u>QGFTGK	60				47		55		48
Triosephosphate isomerase	P17751	IAVAAQN<u>C</u>YK	67	1	40	1.61	48	1.81^{*}	46	$0.68^{*,\dagger,\ddagger}$	42
		IIYGGSVTGAT<u>C</u>K	218	1	103	2.88^{*}	103	2.33^{*}	98	$1.04^{\dagger,\ddagger}$	90
Aconitate hydratase (M)	Q99KI0	VGLIGS<u>C</u>TNSSYEDMGR	385	1	132	2.88	128	2.03^{*}	137	$0.95^{\ddagger}$	128
Aspartate aminotransferase	P05201	INM<u>C</u>GLTTK	391								
Aspartate aminotransferase (M)	P05202	VGAFTVV<u>C</u>K	295	1	95	1.29^{*}	99	1.70^{*}	97	$1.30^{*,\ddagger}$	115
β-enolase	P21550	VNQIGSVTESIQA<u>C</u>K	357	1	128	1.35^{*}	115	1.71^{*}	123	$0.69^{*,\dagger,\ddagger}$	123
Cysteine and glycine-rich protein 3	P50462	TVYHAEEIQ<u>C</u>NGR	25	1	72	2.49	84	1.61^{*}	73	$0.61^{*,\ddagger}$	87
Cysteine-rich protein 2	Q9DCT8	ASSVTTFTGEPNM<u>C</u>PR	126	1	89	2.27^{*}	90	1.74^{*}	88	$1.04^{\dagger,\ddagger}$	98
Cytochrome c oxidase subunit 5b (M)	P19536	cPN<u>C</u>GTHYK	115						33		
Electron transfer flavoprotein subunit α (M)	Q99LC5	TIYAGNAL<u>C</u>TVK	155	1	63	2.38	108	3.87	67	0.96	65
Electron transfer flavoprotein subunit β (M)	Q9DCW4	EIIAVS<u>C</u>GPSQ<u>C</u>QETIR	66,71	1	124	1.01	107	1.42^{*}	127	$0.44^{\ddagger}$	128
Enoyl-CoA hydratase (M)	Q8BH95	LVEEAIQ<u>C</u>AEK	225	1	88	6.06^{*}	92	7.28^{*}	86	$2.24^{\dagger,\ddagger}$	78
Isocitrate dehydrogenase [NAD] subunit α (M)	Q9D6R2	IEAA<u>C</u>FATIK	331				56		57		
Long-chain-fatty-acid-CoA ligase 1	P41216	GIQVSNNGP<u>C</u>LGSR	109								
Metallothionein-1	P02802	S<u>CC</u>S<u>CC</u>PVG<u>C</u>SK	33,34,36 37,41								
		GAADK<u>C</u>T<u>CC</u>A	57,59,60								
NADH dehydrogenase [ubiquinone] 1 α subcomplex subunit 10 (M)	Q99LC3	VITVDGNI<u>C</u>SGK	67	1	61	1.31	67	1.45^{*}	70	$1.30^{\ddagger}$	68
Peroxiredoxin-6	O08709	DFTPV<u>C</u>TTELGR	47	1	67	8.47^{*}	71	9.17^{*}	65	$5.11^{*,\dagger,\ddagger}$	65
Propionyl-CoA carboxylase α chain	Q91ZA3	MADEAV<u>C</u>VGPAPTSK	107								
Succinate dehydrogenase [ubiquinone] flavoprotein (M)	**Q8K2B3**	VGSVLQEG<u>C</u>EK	536								
Succinyl-CoA ligase subunit β (M)	Q9Z2I9	ILA<u>C</u>DDLDEAAK	430	1	75	4.50^{*}	69	5.38^{*}	77	$1.71^{*,\dagger,\ddagger}$	75
Sarcoplasmic/endoplasmic reticulum calcium ATPase 2	O55143	SMSVY<u>C</u>TPNKPSR	498	1	57	2.98	65	1.36	55	1.31	59
Tubulin β-4 chain	**P04350**	NMMAA<u>C</u>DPR	303	1	62	3.28^{*}	59	1.60^{*}	64	$0.36^{*,\dagger,\ddagger}$	62
		TAV<u>C</u>DIPPR	354	1	53			2.05^{*}	52	$1.35^{\ddagger}$	52
Very long-chain specific acyl-CoA dehydrogenase (M)	P50544	SSAIPSP<u>C</u>GK	238	1	35	4.00^{*}	42	$1.17^{\dagger}$	39	$0.39^{*,\dagger}$	40
Voltage-dependent anion channel protein 2 (M)	Q60930	S<u>C</u>SGVEFSTSGSSNTDTGK	48	1	122	3.24^{*}	127	$2.11^{*,\dagger}$	131	$1.50^{\dagger,\ddagger}$	137

Proteins selected for inclusion in Online Table I are the same proteins from Table 1. Each protein/peptide was identified from at least three of five SNO-RAC/LC-MS/MS proteomic analyses (peptides were filtered at a false discovery rate of 5%; peptides with ion scores below 30 were not accepted). (M): mitochondrial isoform; (<u>C</u>): SNO cysteine residue; (c): NEM-blocked cysteine residue; Peptides not detected under the specified condition contain a blank space in the ion score column. Peptide quantitative ratio was determined via label-free peptide analysis. $^{*}p<0.05$ vs. Perfusion; $^{\dagger}p<0.05$ vs. IPC; $^{\ddagger}p<0.05$ vs. IR.

Additional Online Table Legends

Online Table II. **Oxidized protein/peptide identifications from perfusion hearts as identified via Ox-RAC proteomic analysis.** LC-MS/MS derived peptide sequences and MASCOT MS2 search identifications (false discovery rate of 5%). Peptide identifications with ions scores below 30 were not accepted; non-cysteine containing peptides were filtered from the data set. To view peptide sequences, click on the '+' symbol found on the left side of the spreadsheet. Each of 5 biological replicates was run in order to increase protein/peptide identifications; replicates are identified in column headings as A2 (Perfusion Heart 1), B2 (Perfusion Heart 2), C2 (Perfusion Heart 3), D2 (Perfusion Heart 4), and E2 (Perfusion Heart 5). Please note that Online Table II includes all Ox-RAC protein/peptide identifications from perfusion hearts, including those observed in fewer than three of five Ox-RAC proteomic analyses.

Online Table III. **Oxidized protein/peptide identifications from IR hearts as identified via Ox-RAC proteomic analysis.** LC-MS/MS derived peptide sequences and MASCOT MS2 search identifications (false discovery rate of 5%). Peptide identifications with ions scores below 30 were not accepted; non-cysteine containing peptides were filtered from the data set. To view peptide sequences, click on the '+' symbol found on the left side of the spreadsheet. Each of 5 biological replicates was run in order to increase protein/peptide identifications; replicates are identified in column headings as A2 (IR Heart 1), B2 (IR Heart 2), C2 (IR Heart 3), D2 (IR Heart 4), and E2 (IR Heart 5). Please note that Online Table III includes all Ox-RAC protein/peptide identifications from IR hearts, including those observed in fewer than three of five Ox-RAC proteomic analyses.

Online Table IV. **Oxidized protein/peptide identifications from IPC hearts as identified via Ox-RAC proteomic analysis.** LC-MS/MS derived peptide sequences and MASCOT MS2 search identifications (false discovery rate of 5%). Peptide identifications with ions scores below 30 were not accepted; non-cysteine containing peptides were filtered from the data set. To view peptide sequences, click on the '+' symbol found on the left side of the spreadsheet. Each of 5 biological replicates was run in order to increase protein/peptide identifications; replicates are identified in column headings as A2 (IPC Heart 1), B2 (IPC Heart 2), C2 (IPC Heart 3), D2 (IPC Heart 4), and E2 (IPC Heart 5). Please note that Online Table IV includes all Ox-RAC protein/peptide identifications from IPC hearts, including those observed in fewer than three of five Ox-RAC proteomic analyses.

Online Table V. **Oxidized protein/peptide identifications from IPC-IR hearts as identified via Ox-RAC proteomic analysis.** LC-MS/MS derived peptide sequences and MASCOT MS2 search identifications (false discovery rate of 5%). Peptide identifications with ions scores below 30 were not accepted; non-cysteine containing peptides were filtered from the data set. To view peptide sequences, click on the '+' symbol found on the left side of the spreadsheet. Each of 5 biological replicates was run in order to increase protein/peptide identifications; replicates are identified in column headings as A2 (IPC-IR Heart 1), B2 (IPC-IR Heart 2), C2 (IPC-IR Heart 3), D2 (IPC-IR Heart 4), and E2 (IPC-IR Heart 5). Please note that Online Table V includes all Ox-RAC protein/peptide identifications from IPC-IR hearts, including those observed in fewer than three of five Ox-RAC proteomic analyses.

Supplemental References

1. Lin J, Steenbergen C, Murphy E, Sun J. Estrogen receptor-beta activation results in S-nitrosylation of proteins involved in cardioprotection. *Circulation.* 2009;120:245-254.

2. Sun J, Morgan M, Shen RF, Steenbergen C, Murphy E. Preconditioning results in S-nitrosylation of proteins involved in regulation of mitochondrial energetics and calcium transport. *Circ Res.* 2007;101:1155-1163.

3. Forrester MT, Thompson JW, Foster MW, Nogueira L, Moseley MA, Stamler JS. Proteomic analysis of S-nitrosylation and denitrosylation by resin-assisted capture. *Nat Biotechnol.* 2009;27:557-559.

4. Perkins DN, Pappin DJ, Creasy DM, Cottrell JS. Probability-based protein identification by searching sequence databases using mass spectrometry data. *Electrophoresis.* 1999;20:3551-3567.

5. Wang G, Wu WW, Zeng W, Chou CL, Shen RF. Label-free protein quantification using LC-coupled ion trap or FT mass spectrometry: Reproducibility, linearity, and application with complex proteomes. *J Proteome Res.* 2006;5:1214-1223.

6. Padgett CM, Whorton AR. S-nitrosoglutathione reversibly inhibits GAPDH by S-nitrosylation. *Am J Physiol.* 1995;269:C739-C749.